Shake table tests of suspended ceilings to simulate the observed damage in the M_S7.0 Lushan earthquake, China

Wang Duozhi, Dai Junwu, Qu Zhe, Ning Xiaoqing

Key Laboratory of Earthquake Engineering and Engineering Vibration, Institute of Engineering Mechanics, China Earthquake Administration, Harbin 150080, China

Abstract: Severe damage to suspended ceilings of metal grids and lay-in panels was observed in public buildings during the 2013 M_S7.0 Lushan earthquake in China. Over the past years, such suspended ceilings have become a common practice in the public buildings in China, including governmental offices, schools and hospitals. To investigate the damage mechanism of the suspended ceilings, a series of three-dimensional shake table tests was conducted to reproduce the observed damage, which is the first shake table test on suspended ceilings in China. A full-scale reinforced concrete frame was constructed as the testing frame for the ceiling, which was single-story and infilled with brick masonry walls to represent the local construction of low-rise buildings. In general, the tested ceiling exhibited similar damage phenomena to the field observation, which was featured by the higher vulnerability of perimeter elements and extensive damage to the cross runners. However, it exhibited lower fragility in terms of peak ground/roof accelerations at the initiation of damage. Further investigations are needed to clarify the reasons.

Keywords：Suspended ceiling; Lushan earthquake; Wenchuan earthquake; Shake table test; Wall closure; Acoustic mineral fiber panel.

1. Introduction

The seismic performance of suspended ceilings has been investigated for decades in major earthquake-prone regions in the worlds. In addition to the limited numerical studies (Yao 2000, Echevarria et al. 2012), experimental tests, especially shake table tests, have been conducted for both industrial qualification and academic research purposes. The first shake table tests on suspended ceilings can be traced back to the early 1980s, in which suspended ceilings of lay-in panels and inverted-T grids hung on specifically designed testing frames were subjected to either earthquake or sinusoidal dynamic loadings (ANCO 1983, Rihal et al. 1984). With the increasing interests on the performance-based earthquake engineering in the late 1990s, the widespread seismic damage to suspended ceilings and the resultant economic loss in moderate to major earthquakes became a major concern for enhancing the resiliency of buildings. This stimulated more shake table tests in the 21st century to understand the influential factors of ceiling damage and to evaluate the fragility of suspended ceilings for the purpose of seismic performance assessment of buildings.

Yao (2000) conducted a series of unidirectional shake table tests on direct hung suspended ceiling systems in Taiwan. The systems tested were similar to the commercial ceiling systems in the U.S., which are typically composed of main/cross runners with inverted tee sections, perimeter angles (wall closures), lay-in panels and suspension wires. In seismic regions, pop rivets at the two adjacent wall edges and splay wires are also required. The test results showed that the perimeter pop rivets and transverse supports could increase the ceiling's seismic capacity whereas splay wires were ineffective in mitigating ceiling damage. The test results were also correlated to the observed ceiling

damage in a M6.2 earthquake in Taiwan.

Numerous shake table tests have been carried out in the U.S. on similar ceiling systems. Many of the tests were for commercial uses and only a few were published (Badillo-Almaraz et al. 2007, Gilani et al. 2010, Ryu et al. 2012, Soroushian et al. 2015a). Although the ceiling systems were fundamentally the same in these tests, the effects of different details and configurations, such as the splay wires, compression posts, pop rivets, seismic clips, types of tiles, ceiling areas and multi-directional motions, were examined. The required response spectra in AC156 (ICC, 2012 or its previous editions) were generally followed in defining the input time history, which was supposed to represent floor motions rather than ground motions. Specifically-designed steel braced frames were usually mounted on the shake table to suspend the ceilings. These test frames were required to exhibit high frequency to avoid amplifications of the table motion in the frequency range of interest. Similar tests were conducted on various ceiling systems in other parts of world, such as the similar system in New Zealand (Pourali et al. 2015), the suspended continuous ceiling in Italy (Magliulo et al. 2012) and the curved ceiling with channel grids for large open space in Japan (Watakabe et al. 2012).

A more straightforward way of generating floor motions as input for the ceilings is to test in full-scale multi-story buildings. This was done by Soroushian et al. (2012) on a 5-story steel moment frame in E-Defense. Ceiling systems of the U.S. practice were installed on the 4^{th} and 5^{th} floor of the building. A sprinkler system was also installed together with the ceiling to see their interaction. Similar to the past lab observations, splay wires and compression posts seemed not effect in mitigating ceiling damage. On the same building, suspended ceilings of Japanese practice were also tested (Hoehler et al. 2012). The Japanese system differs from the U.S. system in several ways: (1) threaded rods rather than wires are preferred for suspension of the T-sectioned grid; (2) lateral restraints are provided by diagonal metal braces in both ways instead of splay wires; (3) sufficiently large gap (200 mm in the test) is provided at the perimeter of the ceiling to avoid any contact with the walls.

Although widely used in public and commercial buildings, the suspended ceilings in China have not been carefully examined regarding their seismic performance. Nonstructural components such as masonry infills and suspended ceilings were extensively damaged during the 2008 M8.0 Wenchuan earthquake in China (Liu and Jiang, 2013). However, the collapse of numerous buildings that lead to tremendous loss of lives in the earthquake drew people's attentions away from the nonstructural problems. It was not until the 2013 M7.0 Lushan earthquake in the same region that the nonstructural damage emerged as a major concern to the building research community in China.

In the following sections, the Chinese current practice of suspended ceilings is first introduced. Then the ceiling damage observed in the 2013 Lushan earthquake in China is summarized, and the results of a shake table test to simulate the observed damage are presented, which is the first shake table test on suspended ceilings in China.

2 The current practice of suspended ceilings in public buildings in China

2.1 Seismic design requirements

Seismic provisions for non-structural components was first introduced to the Chinese seismic design code for buildings (GB50011-2001) in 2001. The code was revised in 2010 to address the findings in the deadly Ms8.0 Wenchuan earthquake two years earlier, whereas the nonstructural provisions were left unchanged (GB50011-2010).

In the code, a small chapter of seven pages is devoted to nonstructural components, in which an equivalent lateral force method is introduced for components other than heavy or flexibly-supported equipment. The seismic design force on the center of gravity of the component, F, is calculated by Equation (1). Only horizontal seismic force need to be taken into account.

$$F = \gamma\eta\zeta_1\zeta_2\alpha_{\max}G \tag{1}$$

where γ is the function modification factor that varies from 0.6 to 1.4, depending on the occupancy category of the building and the performance objective of the component; η is a material modification factor that takes values between 0.6 and 1.2; ζ_1 is the component status factor, taking the value of 1.0 for rigid or rigidly attached components (fundamental period less than 0.06 s), and 2.0 for flexible or flexibly attached components. It is the same in concept with the component amplification factor, a_p, in ASCE 7 (American Society of Civil Engineers, 2010); $\zeta_2 = 1+z/h$ is the component location factor, where z is the height of the attachment point of the component with respect to the base and h is the roof height of the structure; $\alpha_{\max}$ is the reduced short-period spectral acceleration, which is similar to S_{DS}/R_p in ASCE 7 (S_{DS}: design spectral acceleration at short period; $R_p = 2.5$ for ceilings is the component response modification factor); G is the component's operating weight.

The occupancy category, which is based on the Standard for Classification of Seismic Protection of Building Construction (GB50223-2008), is similar in concept to the risk category in ASCE 7 (ASCE, 2010) but different in specific definitions. Category I include essential facilities, the failure of which could pose a substantial threat to the public safety of the community; category II include buildings that require immediate occupancy after an earthquake, or that could pose a substantial risk to human lives, such as hospitals, emergency reaction centers, large power plants, etc; category IV includes buildings that represent a low risk and the seismic design requirement of which could be loosened; category III includes all buildings except those listed in other categories of higher or lower risks.

The code-suggested values of the modification factors, η and γ, for ceilings are listed in Table 1. Only the categories II and III are included in Table 1. For buildings in category I, the design of its nonstructural components should be subjected to specific study. On the other hand, seismic design is unnecessary for the nonstructural components in buildings of category IV. It is also worth noting that these factors are assigned to the anchorage of the ceiling, rather than the ceiling itself. As stated at the beginning of the nonstructural chapter of the code, it focuses only on the connections between nonstructural components and the structure, rather than the nonstructural components themselves (GB50011-2010). In actual engineering practice, suspended ceilings in China are rarely subjected to seismic design, neither are their anchorage.

Table 1. Modification factors in equivalent lateral force method for ceilings (GB50011-2010)

Component	η	γ	
		Occupancy category II	III
Anchorage for fireproof ceiling	0.9	1.0	1.0
Anchorage for non-fireproof ceiling	0.6	1.0	0.6

2.2 Construction practice

As an industry standard practice, acoustical mineral fiber panels are widely used in suspended ceilings of government-sponsored public buildings in recent years. The ceiling panels are laid in metal grids consisting of main and cross runners of inverted-T sections (Figure 1). Main runners are hung on threaded rods via metal hooks. These suspension rods are anchored in top floor slab by expansion screws. As required by CIBSDR (2012), a collection of industrial standard drawings of suspended ceilings, the spacing of the suspension rods should be no more than 1200 mm in both directions and the distance of the closest rods to the perimeter walls should be no greater than 150 or 200 mm depending on applications.

On the edge of the ceiling, main or cross runners are placed on closure angles that are screwed to the perimeter walls (Figure 1). Pop rivets are not used. Closure angles are supposed to carry only the vertical load of the ceiling, and no lateral resistance exists between grid members and closure angles except for the friction which could be negligibly small.

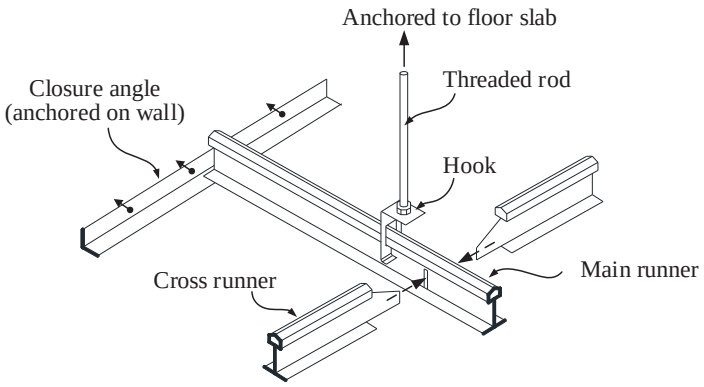

Fig.1 Basic components of ceiling grids

Although not mandated by the seismic code, seismic clips for ceilings of buildings in seismic regions appear in CIBSDR (2012) as shown in Figure 2. Such clips are expected to substantially enhance either the connection to perimeter walls or the integrity of ceiling grids. Unfortunately, they have not yet become a common practice in China, and were not seen in the suspended ceilings in the investigated buildings after the Lushan earthquake. In addition, splay wires and compression posts in the U.S. systems for seismic regions are also uncommon in the Chinese practice.

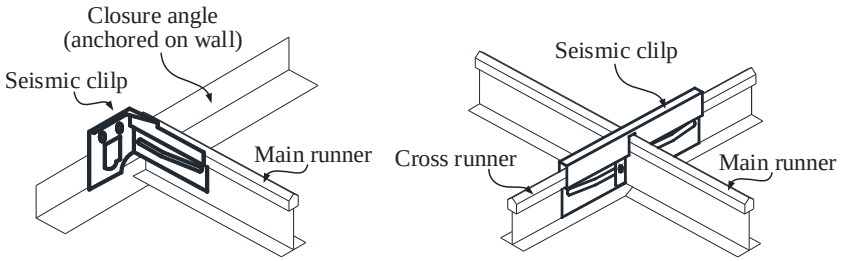

Fig.2 Seismic clips for suspended ceiling grids (reproduced based on CIBSDR, 2012)

3 The observed damage to suspended ceilings during the Lushan earthquake

In April 20, 2013, an M_S7.0 earthquake struck the western Sichuan province in China. The epicenter was located in the town of Longmenshan, which is approximately 20km to the northeast of the city of Lushan. As of April 24, 2013, 196 people were killed, 21 missing and 11470 injured during the earthquake (CEA, 2013a). Several reconnaissance reports are available online for general

information regarding the seismology and impacts of the earthquake (e.g., EERI 2013, Wang and Mooney 2013, Xiong et al. 2013). Figure 3 shows the active faults and major cities near the epicenter on the seismic intensity map released by China Earthquake Administration (CEA, 2013b). The seismic intensity was measured on a scale from I (not felt) to XII (total destruction) in accordance with 'The Chinese Seismic Intensity Scale' (GB/T 17742-2008, 2008), which is based on the Modified Mercalli Intensity scale. In the Lushan earthquake, the highest intensity was IX and the area of intensity IX was approximately 208 km^2.

Unlike the devastating Wenchuan earthquake in the same region five years earlier (Zhao et al. 2009), the Lushan earthquake caused much less structural damage. In addition to the smaller magnitude and the less demanding ground motions, this can be partly attributed to the the enhanced structural performance of the local buildings in the reconstruction after the Wenchuan earthquake. However, in contrast to the satifying performance of the building structures, the extensive damage to nonstructural components such as masonry infills, equipments and suspended ceilings, caused significant ecnomonic losses and delayed the post-quake recovery of the affected region.

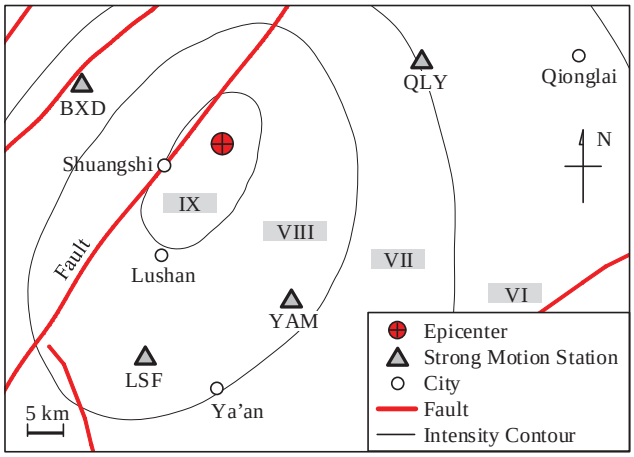

Fig.3 The intensities and strong motion stations in the near field region of Lushan earthquake (reproduced based on Qu et al, 2015)

In particular, damage to suspended ceilings were found in most investigated public buildings ranging from single- or two-story low-rise reinforced concrete (RC) frames or masonry structures to multi-story RC frames for governmental offices, schools and hospitals (Figure 4). The extents of damage varied from complete collapse to sparse falling of ceiling panels. In slightly or moderately damaged ceilings, the perimeter panels seemed most likely to fall as a result of either the dislocation of closure angles (Figure 5) or the falling of main or cross runners from closure angles (Figure 6). This observation is consistent with the damage observed in the past earthquakes (ANCO 1983, Yao 2000). In some cases, closure angles were anchored in nonstructural partitions made of hollow bricks, which were highly vulnerable to seismic shaking. The cracking or distortion of such partitions would at the same time cause damage to the closure angles, triggering the falling of perimeter panels of the suspended ceiling, as is shown in Figure 6(b).

(a) (b)

Fig. 4 Collapse ceilings in (a) the main meeting room of Lushan Radio and TV Center and (b) a classroom in Gaohe Middle School, Qionglai.

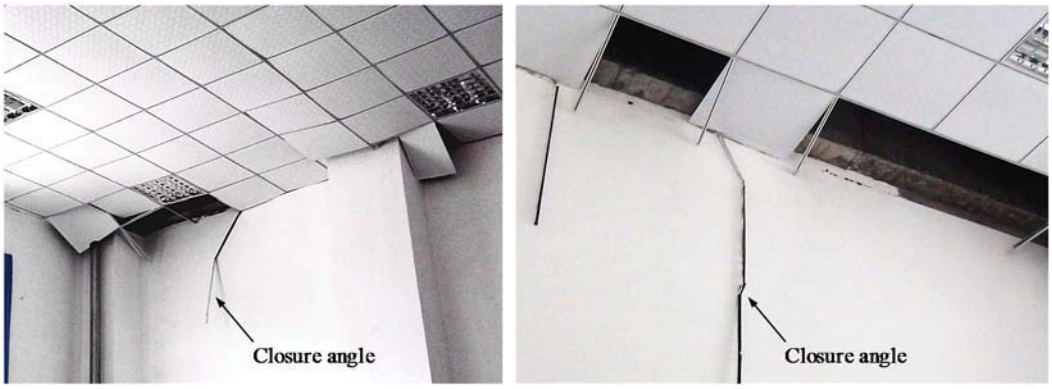

Fig. 5 Dislocated closure angles in Daxing Middle School, Ya'an.

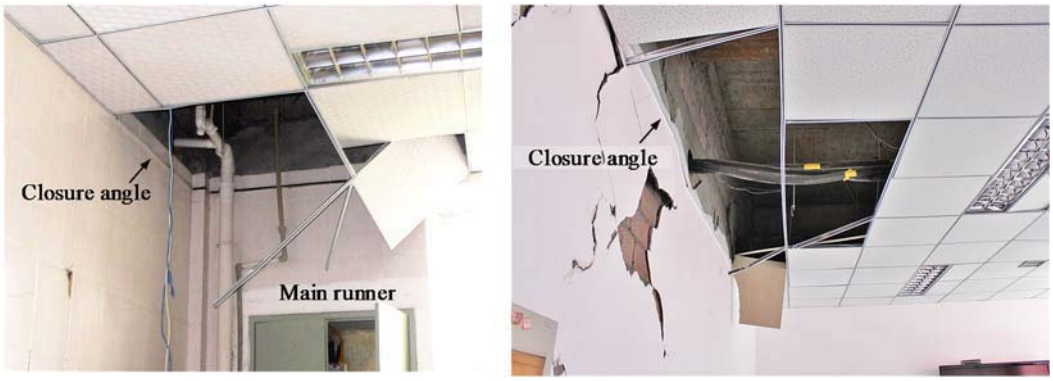

(a) (b)

Fig. 6 Main and cross runners fallen from closure angles in (a) Lushan People's Hospital and (b) Lushan Radio and TV Center.

Damage to cross runners were also commonly-seen. In cross-to-main runner joints without seismic clips, cross runners are very likely to dislocate from main runners (Figure 7(a)). Main runners were usually the last to remain in most investigated ceilings, although the falling of main beams as is shown in Figure 7(b) was also observed in some cases.

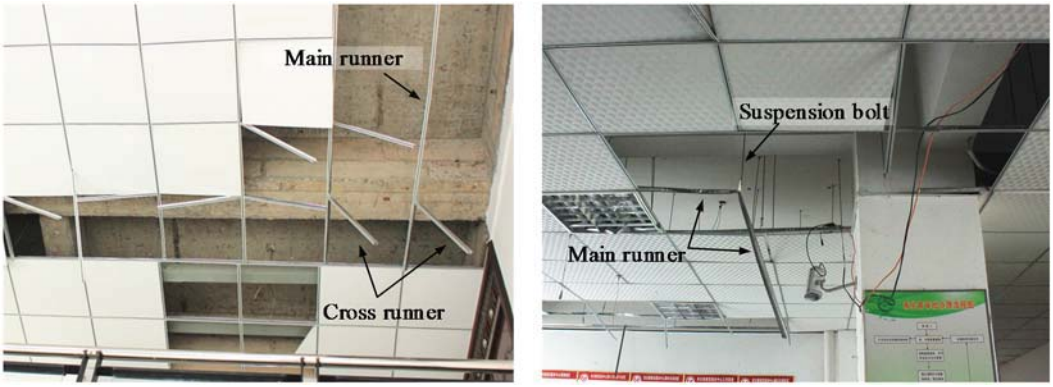

(a) (b)

Fig. 7 (a) Cross runners dislocated from main runners in Lushan Forestry Administrain Office and (b) dislocated and wrenched main runner in Governmental Office of Shuangshi Town.

4. Shake table test program

4.1 Specimen

A shake table test program was conducted to better understand the wide-spread damage to suspended ceilings in the Lushan earthquake. A full-scale single-span single-story RC frame infilled with clay brick walls was designed and constructed as the testing frame to which the ceiling was hung. The plan layout and dimensions of the RC frame are shown in Figure 8. The elevations of the frame model are depicted in Figure 9. The RC frame was not intended to sustain considerable damage throughout the loading. It was designed as a single degree of freedom system with 6.4-ton lumped mass, including the floor slab, the suspended ceiling, the beams and half the columns. The RC columns and beams were thus proportioned that the yield strength of the frame alone would exceed the inertial force of the lumped mass under shakings of 1.0-g peak ground acceleration (PGA). The resultant beam and column cross sectoins are summarized in Figure 8. The 120-mm thick masonry infills would have had a significant contribution to the model's lateral resistance, although it was not taken into account in the design and was considered as a safety margin. The measured fundamental period of the specimen was 0.09 s in the *x*-direction, 0.1s in the *y*-direction and 0.04 s in the *z*-direction.

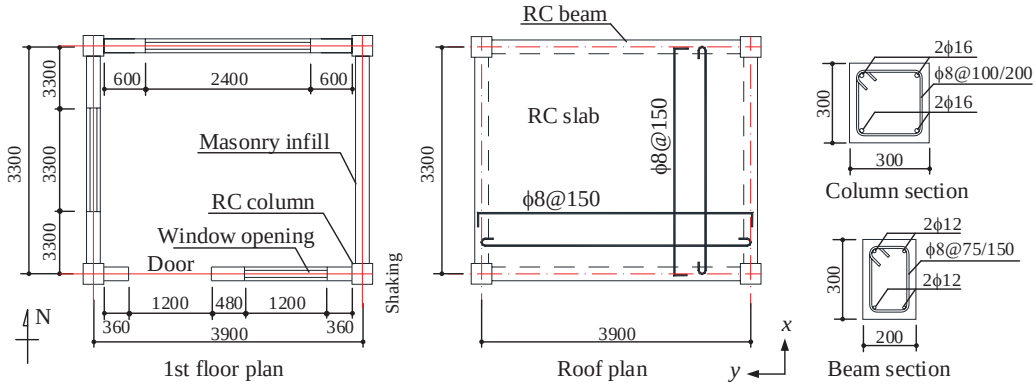

Fig. 8 Structural layout of RC frame for loading

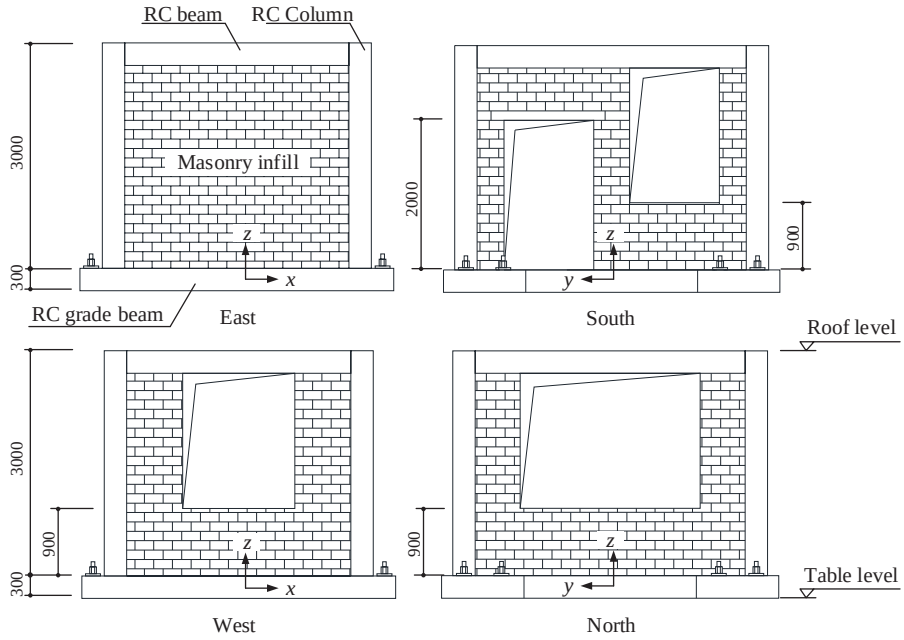

Fig. 9 Elevations of RC frame

(a) Frame model before finishing (b) South façade after finishing (c) Suspended ceiling

Fig.10 The experimental model

The suspended ceiling was installed after the masonry infilled RC frame was completed and the walls finished (Figure 10). The ceiling was 3.1 × 3.7 m in plan as shown in Figure 11. The six main runners were placed at 600 mm distance. Each main runner was hung by three suspension rods at 1200 mm spacing. The ceiling was detailed to conform to the aforementioned common practice and national standards in China with an exception that the outmost suspension points on each main runner were 650 mm to the perpendicular walls, far beyond the 200 mm limit in CIBSDR (2012). This was accepted as a common practice in the real installation of similar suspended ceiling system per the craftsmen's suggestion. The outmost main runners were only 50 mm to the parallel walls, resulting in 50 mm long cross runners spanning between the main runners and the walls. These short cross runners are similar to the helpful transverse supports described by Yao (2000). In the middle of the ceiling, a light fixture was also hung on the floor slab by two suspension wires that penetrated the ceiling panels.

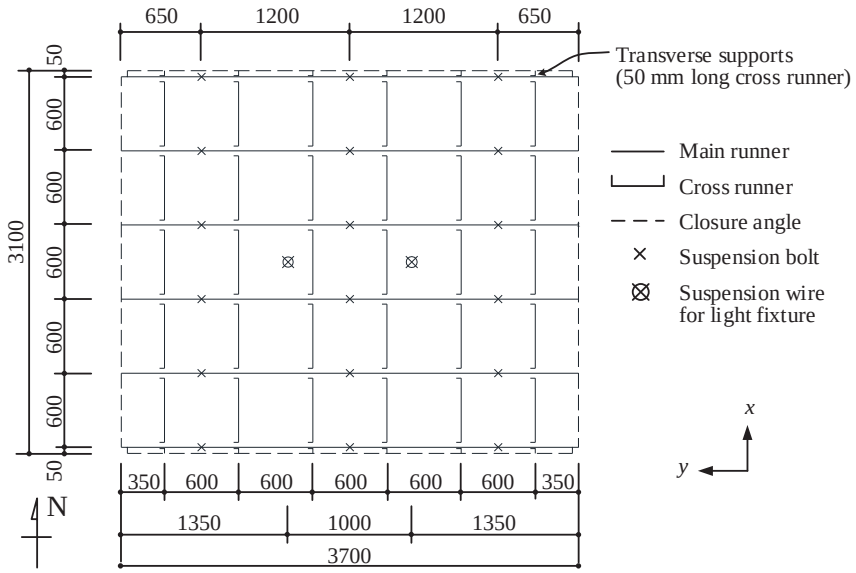

Fig.11 Suspended ceiling layout

12-mm thick mineral fiber acoustical panels with nominal dimensions of 600 × 600 mm were laid in the ceiling grid that was hung 200 mm lower from the bottom of the floor slab by threaded rods. The measured average size of the panels is 595 × 595 mm, and each panel weighed 0.68 kg on average. The metal grid consisted of main runners, cross runners and wall closures as shown in Figure 1. The cross sections and specific dimentions of the grid elements used in the test are given in Figure 12.

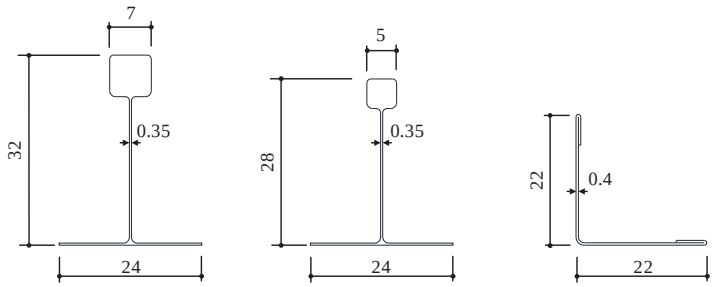

Fig.12 Cross section dimensions of grid components

4.2 Loading control and measurement

The specimen was subjected to nine runs of three-dimensional shaking on a 5×5 m shake table at the Institute of Engineering Mechanics, China. The payload of the shake table is 30 ton, whereas the total mass of the specimen was approximately 20.2 ton. Accelerometers were mounted on top of the RC grade beams and the floor slab to record the three dimensional motion of the specimen. Eight cameras, either inside or outside the specimen, were also installed to record the shaking of the ceiling.

The horizontal peak ground acceleration (PGA) in the controlling direction (*y*-direction, Figure 8) that was obtained by the accelerometers on the grade beams was intended to be incrementally increased from 0.15 g to 1.10 g through the nine runs, as is listed in the second column of Table 2. However, also shown in Table 2, the peak accelerations recorded on the table (i.e., the measured PGAs) more or less deviated from the intended targets. They were generally less than the respective

target. In particular, the measured PGAs in runs 6, 7 and 8 were even smaller than that in run 5, and the relative error of PGA in run 8 was as large as 44%. The maximum PGA achieved in the *y*-direction is 0.85 g in run 9, which was approximately 23% lower than the target. In light of the large deviation from the targets, the test results presented in the following sections should only be interpreted in line with the measured PGAs.

Table 2 Shake table runs and measured peak accelerations (unit: g)

Run	Target PGA-*y*	Measured PGA-*y*		Measured PRA-*y*		Structural Amplification
		As-recorded	Corrected*	As-recorded	Corrected*	
1	0.15	0.13	0.13	0.18	0.18	1.35
2	0.40	0.38	0.37	0.53	0.54	1.44
3	0.60	0.46	0.43	0.72	0.74	1.74
4	0.70	0.68	0.68	1.16	1.12	1.65
5	0.90	0.78	0.77	1.60	1.65	2.15
6	0.90	0.73	0.73	1.45	1.46	2.00
7	1.00	0.73	0.73	1.76	1.77	2.41
8	1.00	0.61	0.56	1.42	1.38	2.43
9	1.10	0.87	0.85	1.96	1.94	2.28

*The record is baseline-corrected and processed by a 4th order Butterworth band-pass filter with a bandwidth of 0.05~50Hz before calculating the peak acceleration.

To simulate the observed damage, it would have been more preferable to use a ground motion record in the 2013 Lushan earthquake as the input time history, during which four strong motion stations (namely, LSF, YAM, QLY and BXD, locations shown in Figure 3) were located within 40 km distance from the epicenter. For some technical reason, however, the technical staff in charge of operating the shake table recommended another strong ground motion record also obtained in western Sichuan province but during the 2008 Wenchuan earthquake (Figure 13) for the table input. Table 3 compares the characteristics of the ground motion records at the aforementioned four stations and those of the measured table motions. They are similar in the low PGV to PGA ratios and short durations, which suggests rich contents in high-frequency domain (McGuire, 1978). Therefore, it was considered practically acceptable to represent the ground motion characteristics of the inspected region. The overall duration of the loading in each run is 30 s.

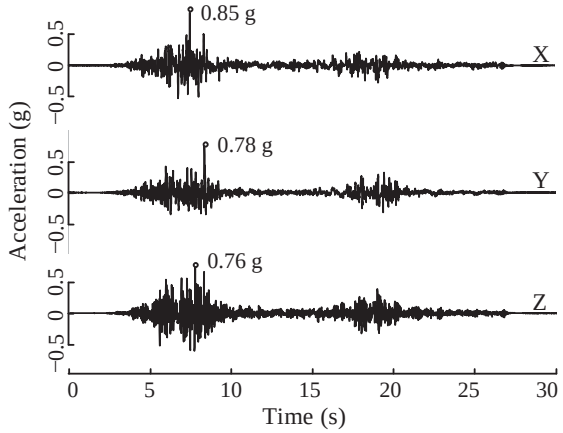

Fig.13 Time history of earthquake motion for input (run 5)

Table 3 Characteristics of recorded motions in Lushan earthquake

Record	PGA(g)		PGV(cm/s)		T_d(s)*
	Horizontal	Vertical	Horizontal	Vertical	
BXD	1.05	0.54	25.8	15.7	5.7
YAM	0.43	0.11	12.3	7.9	25.2
LSF	0.38	0.28	15.3	11.9	23.4
QLY	0.32	0.11	17.9	5.5	13.3
run 5	0.77	0.76	22.8	16.3	14.5
run 9	0.85	0.66	32.3	14.2	14.6

*The significant durations between 5% and 95% earthquake input energy of the corrected records (Trifunac and Brady, 1975).

The rich high-frequency contents are obvious on the response spectra of the input motion. Figure 14 compares the pseudo accelertion spectra of the measured motion at the roof level in run 5 with the requried response spectrum (RRS) prescribed in AC156 (ICC 2012). The response spectra of the table motion differs from the RRS significantly in both the frequency contents and the ratio of horizontal to vertical motions. For periods less than 0.2 s, the response spectra of the horizontal table motions are several times greater than RRS, whereas they are much less than RRS for longer periods. The response spectrum of the vertical table motion is similar to the horizontal ones, whereas the vertical component in RRS is 2/3 of the horizontal ones. These differences should be noted when comparing the current test to other shake table tests in compliance with the AC156 approach.

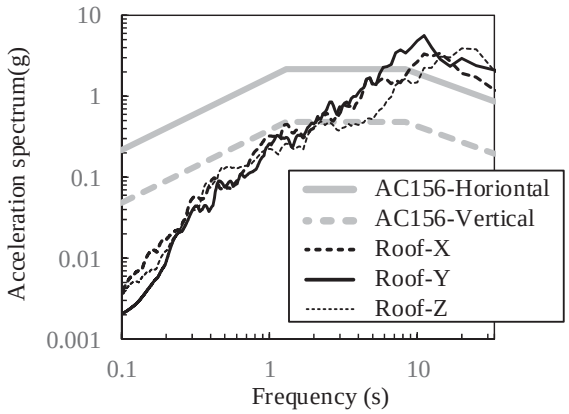

Fig.14 Acceleration spectra of roof motions in run 5 compared with required response spectra in AC156 (2012)

4.3 Test results

The ceiling sustained no obvious damage in the first four runs with PGAs in the *y*-direction from 0.13 to 0.68 g. Figure 15 and Table 4 summarize the damage process of the ceiling in the runs 5 to 9. The damage was inititaed when a cross runner near the southwestern corner fell down at the 6 second in run 5, during which the peak roof acceleration (PRA) reached 1.65 g, and then a 350×600mm edge panel on it fell down 10 seconds later. The absense of the fallen panel immediately allowed the other panels in the same row to slide along the main runners during the remaining shaking of the same run. During the subsequent runs (i.e., runs 6 and 7), in which the

measured PRAs were within ±10% of that in run 5, two more panels fell off in another location following the dislocation of a cross runner. In run 8, although the measured PRA was only 1.38 g, 16% lower than that in run 5, the ceiling seems to have lost much of its integrity and the damage near the southwestern corner in run 5 was dramatically spreaded to one fourth of the ceiling. In run 9 with much higher PRA, the ceiling collapsed as more than half the panels were lost and the light fixture also dropped.

Table 4 also gives the loss ratio of the ceiling panels, which is defined as the ratio of the area of fallen panels to the total ceiling area. Different from the common practice of restoring the ceiling after each run for the purpose of evaluating its fragility, the damaged ceiling components were not replaced so that the damage could be accumulated among the runs in the current test. As a result, the loss ratio is not a monotonic function of the measure PRA in the current test. In particular, the loss ratio kept on increasing even if the PRAs in subsequent runs were smaller than those in previous runs, such as run 6 as compared to run 5, and run 8 as compared to run 7. This suggests a risk for ceiling panels to fall in aftershocks once the integrity of the ceiling was reduced in the main shock.

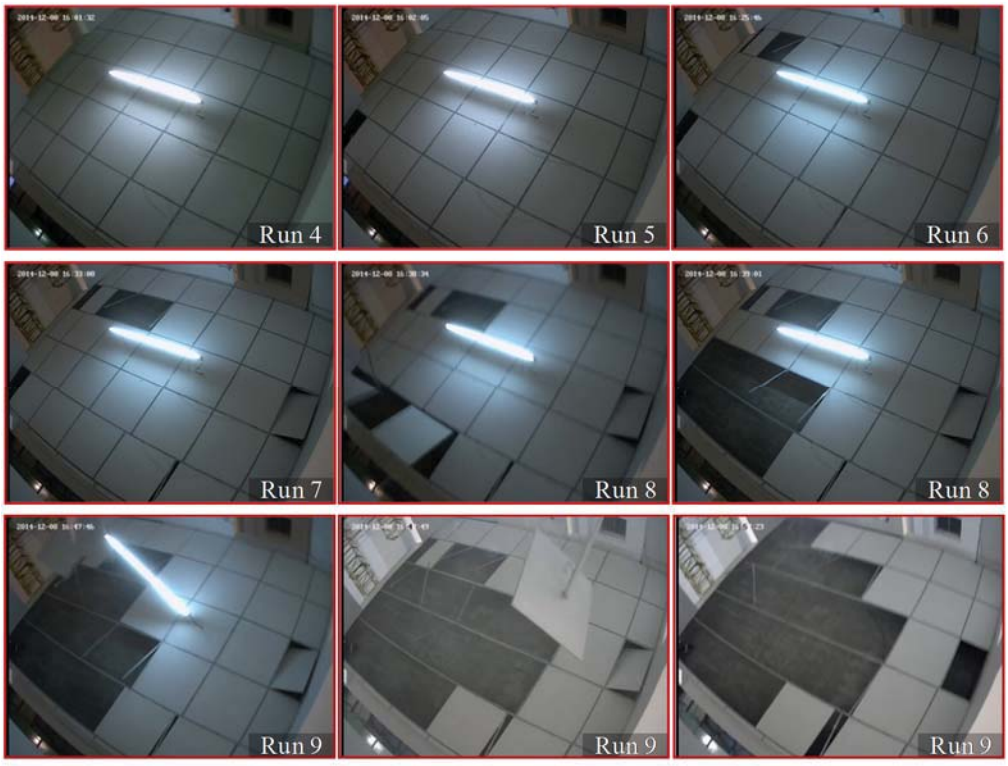

Fig.15 Falling process of ceiling panels

Table 4. Damage to ceilings and loss ratio of ceiling panels

Run	Measured PRA (corrected) (g)	Damage description	Ceiling loss ratio (%)	Incremental loss ratio (%)
5	1.65	A cross runner drops, a panel on the edge falls, panels slide	0.5	0.5
6	1.46	Another cross runner dislocated, another panels fall, more panels slide	2.4	1.8
7	1.77	More cross runners fail, more panels fall,	8.6	6.3

		more significant sliding		
8	1.38	Approximately 1/4 of the cross runners dislocated, more panels fall.	29.3	20.7
9	1.94	Light fixture drops, more cross runner dislocated, more panels fall.	56.5	27.2

Figure 18 compares the pseudo accelertion spectra of the measured table/roof motion in run 5, in which the ceiling damage was initiated, with the design spectrum in the Chinese seismic code for buildings (GB50011-2010) for the city of Lushan. The design floor spectrum in Figure 18(b) was obtained by amplifying the design spectrum for buildings on the ground in accordance to Equation 1, taking $\gamma = 1.0$, $\eta = 0.9$, $\zeta_1 = 1.0$ and $\zeta_2 = 2.0$ (i.e., $z = h$ assumed). At ground levels, the response spectra for periods less than 0.2 s are much greater than the design spectrum. Such rich short-period contents of the table motion were further amplified at the roof level where the ceiling was suspended, because a relatively rigid loading frame (the masonry-infilled RC frame) was used. In this sense, the behavior of the tested ceiling is representive of ceilings in low-rise public buildings of short periods, such as the one- or two-story confined masonry or masonry-infilled RC framed buildings for governmental offices and police stations commonly seen in rural towns.

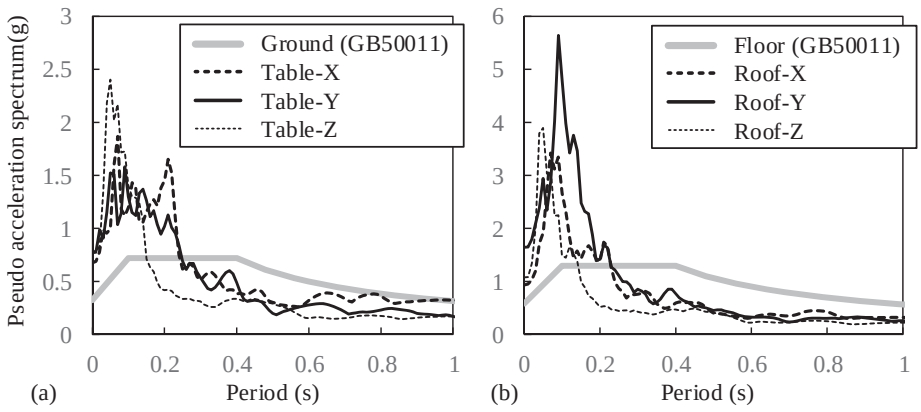

Fig.18 Acceleration spectra of table and roof motions compared with design spectra for Lushan in Chinese seismic code (run 5)

It is also worth noting that the tested ceiling exhibited less fragility than those investigated after the Lushan earthquake. The maximum spectral acceleration at the roof level in run 5, during which the first falling of ceiling panels took place, is 5.6 g, whereas the design floor spectra for Lushan city is only 1.3 g (Figure 18b). In run 5, the PGA was 0.77 g and exceeded the PGAs recorded in the LSF, YAM and QLY stations. Notwithstanding, the observed damage to ceilings in the areas near the three stations was considerably severer than that observed in run 5. This may be attributed to the scale of the specimen. The tested ceiling is much smaller in plan than the ceilings in commonly-seen public buildings. In RC framed public buildings, the span is usually 6 ~ 7 m for office rooms, and even larger for meeting rooms or entrance halls. The size effect was investigated by Ryu et al (2012). In addition, the very short cross runners on both sides of the ceiling may also have increased the capacity of the ceiling, as suggested by Yao (2000). The well-defined conditions and quality control in this particular research work may also result in a ceiling of higher capcity than those in real practice.

Similar to the damage observed after the Lushan earthquake, the joints of cross runners are most fragile in the tested ceiling grid. The joint may fail in horizontal shear under the push of a panel sliding along the main beam, as shown in Figure 16(a). In this case, the latches on both ends of a cross runner would fail at the same time. The cross runner may not fall immediately after the latches are sheared, but the integrity of the ceiling grid is weakened. In other cases, the latch at one end of a cross runner may be sheared off the main runner as shown in Figure 16(b). Soroushian et al (2015b) investigated the axial capacity of the latched joints of cross-to-main runners through static testing. Studies on the out-of-plane shear capacity of the joints have not been reported.

The main runners did not fall throughout the test. Besides, the closure angle in the current test also performed well. Figure 17 shows the only observed damage to the closure angles.

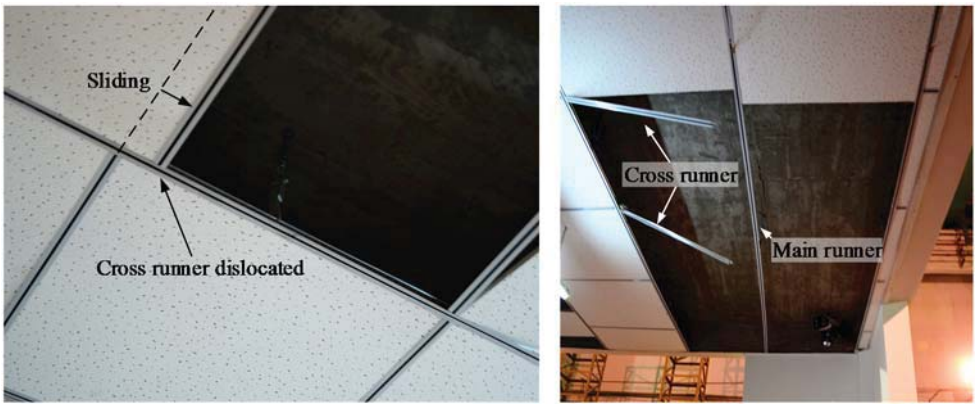

(a) (b)

Fig.16 Damage to cross tees in shake table tests (run 7 and 8)

Fig.17 Damage to perimeter runners in shake table tests (run 5)

5. Conclusions

The suspended ceiling system of lay-in panels and T-sectioned grids is widely used in China, especially in public buildings constructed in recent years. This system is imported primarily from the U.S., although some details are different. However, the seismic design and details of this system are currently absent in China. Ceilings of this system sustained widespread and significant damage during the 2013 Lushan earthquake in southwestern China. Consistent with the observations in past earthquakes in other earthquake-prone regions, the damage to these ceilings during the Lushan earthquake highlighted the vulnerability of perimeter components and cross runners.

To simulate the ceiling damage, a three-dimensional shake table test was conducted on

suspended ceiling of the Chinese routine practice for government-sponsored public buildings, which is the first test of this type in China. The test partially reproduced the observed ceiling damage in the earthquake. It also revealed some damage phenomena that can hardly be observed in the field survey after the quake. Major characteristics of the ceiling damage in the test include: (1) The damage initiated at the corner components and then spread to other parts of the ceiling; (2) The ceiling would lose much of its integrity after the falling of only a few panels; and (3) The cross runners are much more vulnerable than main runners.

However, the ceiling in the lab tests exhibited significantly lower fragility than those in the earthquake in terms of peak ground accelerations. Careful examinations including additional tests are needed to clarify the reasons.

Acknowledgement

The research is sposored by a research fund for earthquake engineering of China Earthquake Administration (201508023), a project of the National Science & Technology Support Program during the Twelfth Five-year Plan Period of China (2015BAK17B03) and a general program of National Natural Science Foundation of China (51578515).

References

ANCO (1983), *Seismic hazard assessment of nonstructural ceiling components - Phase I*, ANCO Engineering, Inc. Culver City, CA.

ASCE (2010), *Minimum Design Loads for Buildings And Other Structures, ASCE/SEI Standard 7-10*, American Society of Civil Engineers, Reston.

Badillo-Almaraz H, Whittaker A.S. and Reinhorn A.M. (2007), "Seismic fragility of suspended ceiling systems," *Earthquake Spectra*, **23**: 21-40.

China Earthquake Administration (CEA) (2013), "*Earthquake Intensity Map of M7.0 '4.20' Lushan Earthquake in Sichuan.*" Released on April 25. (in Chinese)

China Institute of Building Standard Design and Research (CIBSDR) (2012), *Indoor Decoration: suspended ceiling inside, National Standard Design 12J502-2*, Beijing, China Planning Press, pp. 60-113 (in Chinese)

China Strong Motion Networks Center (CSMNC) (2013), http://www.csmnc.net, accessed on May 28, 2013.

Earthquake Engineering Research Institute (EERI), 2013. "The Mw 6.6 Earthquake of April 20, 2013, in Lushan, China, Learning from Earthquakes," available at https://www.eeri.org/wpcontent-/uploads/Lushan-China-Earthquake-Report.pdf.

Echevarria AA, Zaghi AE, Soroushian S, Maragakis EM (2012), "Seismic fragility of suspended ceiling systems," *15th World Conference on Earthquake Engineering*, in CD-ROM, Paper No.4325.

GB50011 (2010), *Code for seismic design of buildings.* (in Chinese)

GB50223 (2008), *Standard for classification of seismic protection of building construction.* (in Chinese)

Gilani A., Reinhorn A., Glasgow B., Lavan O. and Miyamoto H (2010), "Earthquake Simulator Testing and Seismic Evaluation of Suspended Ceilings," *Journal of Architectural Engineering, ASCE*, **16**: 63-73.

Gilani, Amir S. J.; Takhirov, Shakhzod M.; Tedesco, Lee (2012), "Seismic evaluation procedure for suspended ceiling and components new experimental approach," *15th World Conference on Earthquake Engineering*, in CD-ROM, Paper No.0326.

International Code Council (ICC), (2010). *Acceptance criteria for seismic qualification by shake-table testing of nonstructural components and systems*. Rep. No. ICC-ES AC156, ICC Evaluation Service, Inc., Whittier, Calif.

Liu XJ and Jiang HJ (2013), "State-of-the-art of performance-based seismic research on nonstructural components," *Journal of Earthquake Engineering and Engineering Vibration*, **33**(6): 53-62. (in Chinese).

Magliulo G., Pentangelo V., Maddaloni G., Capozzi V., Petrone C., Lopez P., Talamonti R. and Manfredi G (2012), "Shake table tests for seismic assessment of suspended continuous ceilings," *Bulletin of Earthquake Engineering*, **10**: 1819-1832.

Pourali, A., Dhakal, R.P., MacRae, G.A. and Tasligedik, A.S (2015), "Shake table tests of perimeter-fixed type suspended ceilings," *New Zealand Society for Earthquake Engineering Annual Technical Conference*, **O-71**: 648-659.

Qu Z, Dutu A, Zhong JR and Sun JJ (2013), "Seismic damage of masonry infilled timber houses in the 2013 M7.0 Lushan earthquake in China," *Earthquake Spectra*, 2015, **31**(3): 1859-1874.

Rihal, Satwant S. and Granneman, Gary (1984), "Experimental investigation of the dynamic behavior of building partitions and suspended ceilings during earthquakes," *8th World Conference on Earthquake Engineering*, 5: 1135-1142.

Soroushian, S.; Ryan, K.L.; Maragakis, M.; Wieser, J.; Sasaki, T.; Sato, E.; Okazaki, T.; Tedesco, L., Zaghi, A.E.; Mosqueda, G.; Alvarez, D. (2012), "NEES/E-Defense tests: seismic performance of ceiling/sprinkler piping nonstructural systems in base isolated and fixed base building," *15th World Conference on Earthquake Engineering*, in CD-ROM, Paper No.5101.

Soroushian, S, Rahmanishamsi, E, Ryu K P, Maragakis M and Reinhorn, A M. (2015a), "Experimental fragility analysis of suspension ceiling systems," *Earthquake Spectra*, online preprint.

Soroushian, S, Maragakis, M and Jenkins, C. (2015b), "Axial capacity evaluation of typical suspended ceiling joints," *Earthquake Spectra*, online preprint.

Trifunac, M.D. and Brady, A.G. (1975), "A study on the duration of strong earthquake ground motion," *Bulletin of the Seismological Society of America*, **65**(3): 581-626.

Wang, H. L., and Mooney, W. D. (2013), "A Field Assessment of the April 20, 2013, Mw = 6.6, Lushan, China, Earthquake," available at https://www.eeri.org/wp-content/uploads/Mw6.6-Lushan-Earthquake-report1.pdf.

Watakabe, M.; Inai, S.; Ishioka, T.; Iizuka, S.; Takai, S.; Kanagawa, M. (2012), "A study on the

behavior of seismically engineered ceiling systems of large open structures subjected to earthquake excitations," *15th World Conference on Earthquake Engineering*, in CD-ROM, Paper No.2675.

Xiong LH, Lan RQ, Wang YM, Tian XM and Feng B (2013), "Earthquake damage investigation of structures in 7.0 Lushan strong earthquake," *Journal of Earthquake Engineering and Engineering Vibration*, **33**(4): 35-43 (in Chinese).

Yao GC (2000), "Seismic Performance of Direct Hung Suspended Ceiling Systems," *Journal of Architectural Engineering, ASCE*, **6**(1): 6-11.

Zhao, Bin; Taucer, Fabio; Rossetto and Tiziana (2009), "Field investigation on the performance of building structures during the 12 May 2008 Wenchuan earthquake in China," *Engineering Structures*, **31**(8): 1707-1723.